Adsorption isotherms and surface geometry[1]

C. Rascón[2], A. O. Parry[2,3]

[1]Paper presented at the Fourteenth Symposium on Thermophysical Properties, June 25-30, 2000, Boulder, Colorado, U.S.A.

[2]Department of Mathematics, Imperial College, 180 Queen's Gate, London SW7 2BZ, United Kingdom

[3]To whom correspondence should be addressed.

Abstract

We consider fluids adsorbed at generalised wedges described by shape functions x^γ in one direction (x), and translationally invariant in the other. For the limiting cases $\gamma = 0$ and $\gamma = \infty$, the substrate corresponds to a planar wall and a capillary slit respectively. In this way, we show how wetting-like adsorption isotherms become capillary-like as gamma is increased from zero to infinity. The mechanism for the cross-over to condensation is shown to involve several intermediate regimes corresponding to novel examples of adsorption isotherms.

KEY WORDS: capillary condensation; effective interfacial model; interfacial tension; wetting.

1 Introduction

The adsorption properties of planar substrates have been widely studied by means of effective interfacial methods [1]. Within this formalism, the energy of an adsorbed liquid layer of microscopic thickness is given by the functional

$$\mathcal{H}[\ell] = \int d\mathbf{x} \, \left[\, \sigma \sqrt{1 + (\nabla \ell)^2} + W(\ell) + \Delta\mu \, (\rho_L - \rho_G) \, \ell \, \right], \tag{1}$$

where $\mathbf{x}$ represents a point of the substrate, $\ell(\mathbf{x})$ is the thickness of the adsorbed layer at that point, σ is the liquid-gas surface tension, W is an effective potential, $\Delta\mu \equiv \mu_{co}(T) - \mu$ is the chemical potential (measured from the chemical potential at the bulk liquid-gas coexistence), and ρ_L and ρ_G are the densities of the liquid and the gas respectively. Each of the three terms in (1) represents a distinctive contribution to the energy. The first term, involving the gradient, accounts for the area of the liquid-gas interface and is normally approximated for relatively planar interfaces ($|\nabla \ell| \ll 1$) as $(1 + (\nabla \ell)^2)^{1/2} \approx 1 + (\nabla \ell)^2/2$. The interaction of the molecules of the liquid with the substrate is taken into account by the effective potential W, whose analytical form is usually taken to be $W(\ell) \equiv A/\ell^{\,p}$ where A is a Hamaker constant and p accounts for the range of the intermolecular interactions [2]. The third term considers the energy due to the presence of liquid instead of gas, which is the bulk equilibrium phase. By minimising (1) at a constant temperature T ($T_w < T < T_c$ where T_w and T_c are the wetting temperature and the critical temperature respectively), we obtain the mean-field thickness of the adsorbed layer ℓ_π, which is given implictly by $W'(\ell_\pi) + \Delta\mu(\rho_L - \rho_G) = 0$ (the subindex π stands for *planar*). When we approach coexistence at constant temperature T, the thickness of the adsorbed layer diverges continuously with a non-universal exponent β_{co},

$$\ell_\pi \sim \Delta\mu^{-\beta_{co}}, \tag{2}$$

determined by the range of the intermolecular forces, $\beta_{co} = 1/(1+p)$. This phenomenon is commonly known as *complete wetting*.

In the previous discussion we have assumed that the substrate is perfectly *flat*. At present, however, the shape of solid surfaces can be controlled at a mesoscopic level [3], and therefore a further study to determine the role of the surface geometry in adsorption is needed. The strong influence of the substrate geometry on adsorption isotherms is apparent from considering fluid adsorption in a capillary slit, consisting of two parallel flat substrates a distance $\mathcal{L}$ apart. For this system, a different phenomenon, called *capillary condensation*, takes place [4, 5]. By approaching coexistence, microscopic layers of liquid are adsorbed at either wall, following closely the planar law (2). This occurs up to a non-zero value of the chemical potential $\Delta\mu^*$ for which the space between the substrates is abruptly filled with liquid although this phase is *not* thermodynamically stable in bulk. The location of this phase transition is given, for sufficiently large values of $\mathcal{L}$, by the Kelvin equation [4],

$$\Delta\mu^* = \frac{2\,\sigma}{(\rho_L - \rho_G)\,\mathcal{L}} \quad . \tag{3}$$

Capillary condensation is a first-order transition occuring at a *macroscopically* determined phase boundary (for asymptotically large $\mathcal{L}$) and contrasts sharply with the phenomenon of complete wetting at a single substrate which is a second-order transition governed by non-universal critical exponents which depend on the details of the *microscopic* interaction. The purpose of this work is to understand how capillary condensation emerges from the very different phenomenon of complete wetting when we change smoothly the morphology of the confining substrate from a planar wall to a capillary slit.

2 Models for Generalised Wedges

In order to understand the role played by geometry in the adsorption isotherms and the subtle connection between wetting and capillarity, we consider in this paper adsorption at generalised solid wedges with cross section described by a

shape function

$$\psi(x) \equiv \frac{|x|^{\gamma}}{L^{\gamma-1}} \tag{4}$$

in the x direction, where L is a length associated with the dimensions of the wall. These substrate shapes range smoothly between a planar wall for $\gamma = 0$ and a capillary slit of width $\mathcal{L}=2L$ for $\gamma=\infty$ (see Fig. 1). Notable intermediate cases are the linear wedge, $\gamma=1$, and the parabolic wedge, $\gamma=2$. In this system, the equilibrium thickness of the adsorbed layer depends on x. For that reason, previous studies have concentrated on the evolution of the equilibrium thickness at the mid-point ($x=0$), denoted ℓ_0. These studies have been restricted to the particular cases $\gamma=1$ [6, 7, 8, 9], and $\gamma<1$ in the asymptotic limit $\Delta\mu\to 0$ [10] (see below). A short version of this paper has been published elsewhere [11].

2.1 Interfacial Model

In mean-field approaches, the equilibrium interfacial configuration of the adsorbed layer is found from the minimisation of the functional

$$\mathcal{H}[\ell] = \int dx \left[\sigma\sqrt{1+\left(\frac{\partial \ell}{\partial x}\right)^2} + \mathcal{W}_{[\ell,\psi]}(x) + \Delta\mu\,(\rho_L-\rho_G)\,\big(\ell-\psi(x)\big) \right], \tag{5}$$

where the effective potential $\mathcal{W}_{[\ell,\psi]}$ needs to be determined. Two approximations have been mainly used for this effective potential:

- The vertical-distance approximation, also known as Deryagin approximation [12], for which the interaction of the fluid with the substrate is the planar effective potential W evaluated at a thickness given by the local vertical distance between the interface and the substrate; that is, $\mathcal{W}_{[\ell,\psi]}(x) \approx W\big(\ell(x)-\psi(x)\big)$. If the interface is relatively flat, the approximation captures the essential physics of the problem. This method was used in the study of adsorption at the generalised wedge, Eq. (4), for $\gamma<1$ in the asymptotic limit $\Delta\mu\to 0$ (mentioned above)[10]. Only under those particular conditions the interface is flat enough for the approximation to

be valid. The results of that study show that the mid-point thickness ℓ_0 diverges continuously (on approaching coexistence) falling within one of two different regimes depending on the value of γ,

$$\ell_0 \sim \begin{cases} \Delta\mu^{-\beta_0} & 0 \leq \gamma \leq \gamma^* \\ \Delta\mu^{-\frac{\gamma}{2-\gamma}} & \gamma^* \leq \gamma \leq 1. \end{cases} \tag{6}$$

The substrate geometry, therefore, can change the exponent of the divergence from planar (β_0) to geometry dominated ($\gamma/(2-\gamma)$) if the value of γ is larger than the marginal value $\gamma^* \equiv 2\beta_{co}/(1+\beta_{co})$. Alternatively, for a fixed substrate shape, geometry dominates if the range of the forces is smaller than a certain threshold, $p > 2(1-\gamma)/\gamma$. This clearly indicates that for the linear wedge $\gamma = 1$ the divergence is governed by geometry irrespective of the range of the forces. Exact results in 2D linear wedges which include the influence of thermal fluctuation effects beyond the mean-flied approximation show precisely similar behaviour [8].

- The minimum-distance approximation, which improves the previous approximation by evaluating the planar effective potential W at a thickness given by the minimum distance between the interface (at a given point) and the substrate, $\mathcal{W}_{[\ell,\psi]}(x) \approx W\big(d(x)\big)\, \mathcal{J}_{[\psi]}(x)$, with $d(x)^2 \equiv (\ell(x) - \psi(x'))^2 + (x-x')^2$ (where x' minimises $d(x)$ for fixed x) and $\mathcal{J}_{[\psi]}$ being a Jacobian accounting for the non-planarity of the substrate. This method simplifies enormously for the linear wedge, $\psi(x) = \alpha|x|$, yielding [7] $\mathcal{W}_{[\ell,\psi]}(x) \approx \alpha' W\big(\alpha'(\ell(x) - \psi(x))\big)$ with $\alpha' \equiv 1/\sqrt{1+\alpha^2}$, which results in a mere rescaling of the vertical-distance approximation and, for this particular case, produces the same qualitative results as the previous approximation. For an arbitrary wedge, however, this model proved exceptionally complicated and, in turn, does not solve the problem entirely because it breaks down under certain circumstances [13].

In short, neither of these two approximations turns out to be satisfactory for our purposes. It remains an open question whether a particular choice of $\mathcal{W}_{[\ell,\psi]}$ or an extension of the Hamiltonian (5) can be used to describe adsorption at the generalised wedges of Eq. (4) in full, or a density functional description [1] is inevitable.

2.2 Macroscopic Approach

Since the effect of geometry is very dominant in the regime $\gamma \geq \gamma^*$, it is reasonable to assume that the interaction of the fluid layer with the substrate (the term $\mathcal{W}_{[\ell,\psi]}$) can be treated perturbatively since, in this regime, is is small compared to the others (in some sense). Therefore, a macroscopic description of the problem (ignoring microscopic interacting forces) should give us at least a hint of the behaviour of the system. This suggests the approximation $\mathcal{W}_{[\ell,\psi]} \approx \Theta^*\big(\ell(x) - \psi(x)\big)$, where $\Theta^*(\ell) = 0$ for $\ell \geq 0$ and $\Theta^*(\ell) = \infty$ for $\ell < 0$, which is equivalent to considering either of the two approximations (mentioned above) in the limit of extremely weak forces, $p \to \infty$ or $A \to 0$. Minimisation of (5) in this case, can be related to an elegant and a simple geometrical construction. A cylinder whose radius is Laplace's radius of curvature,

$$R_\mu \equiv \frac{\sigma}{(\rho_L - \rho_G)\Delta\mu}, \tag{7}$$

is fitted at the point of maximum curvature of the wedge. The tangency points are the edges of a longitudinal meniscus, whose shape is the lower part of the cylinder (see Fig. 2).

Three important features emerge from this approach:

- The asymptotic behaviour of the interface height on approaching coexistence can be classified into two different regimes, both determined by the

shape parameter γ:

$$\ell_0 \sim \begin{cases} \Delta\mu^{-\frac{\gamma}{2-\gamma}} & 0 \leq \gamma \leq 1 \\ \\ \Delta\mu^{-\gamma} & 1 \leq \gamma. \end{cases} \tag{8}$$

We will refer to the regime characterised by the exponent $\gamma/(2-\gamma)$ as G_1. The regime characterised by the exponent γ, denoted as G_2, is arbitrarily sensitive to changes in the chemical potential $\Delta\mu$ as the exponent can be increased without bound by changing the geometry of the surface. Note that the planar regime (PL) is missing in this approach (compare with (6)) as it has been preempted by the regime G_1 (since $p \to \infty$ implies $\gamma^* \to 0$).

- Two different situations are found regarding the formation of the meniscus. If the cross-section shape $\psi(x)$ is singular at a particular point (in the sense that the second derivative $\psi''(x)$ is discontinuous), a meniscus forms at that point for every value of the chemical potential $\Delta\mu > 0$. This is the case for $\gamma < 2$. In contrast, if the surface is smooth ($\psi''(x)$ is continuous), as happens for $\gamma \geq 2$, no meniscus is formed while the chemical potential difference $\Delta\mu$ is greater than a certain threshold given implicitly by

$$R_\mu < \mathcal{R}(\hat{x}), \tag{9}$$

where $\mathcal{R}(x) \equiv \left(1 + \psi'(x)^2\right)^{3/2}/\psi''(x)$ is the radius of curvature of the surface at the point x and $\mathcal{R}'(\hat{x}) = 0$. In this case, the appearance of a meniscus constitutes a high-order phase transition which we refer to as the *meniscus transition*. But the phenomenology is still richer. For $\gamma > 2$ the equation $\mathcal{R}'(\hat{x}) = 0$ presents two symmetrical solutions and, therefore, *two* symmetrical menisci form. If this happens, as the menisci increase in size by approaching coexistence, a further high-order phase transition is expected when both menisci merge into a unique central meniscus. This second transition, which (for obvious reasons) we refer to as the *Moses*

transition, occurs for a chemical potential given implicitly by

$$R_\mu = \psi(\bar{x}) + \frac{\bar{x}}{\psi'(\bar{x})}, \tag{10}$$

where $\bar{x}$ is a non-zero solution of $\bar{x}\sqrt{1+\psi'(\bar{x})^2} = \bar{x} + \psi(\bar{x})\psi'(\bar{x})$. Decreasing $\Delta\mu$ further drives the system into the geometry-dominated regime G_2 which, as mentioned, is arbitrarily sensitive to changes in $\Delta\mu$. Notice that, in the limit $\gamma \to \infty$, this transition becomes capillary condensation: the merging of the two menisci precipitates the immediate and abrupt rise of the liquid level and the space between the walls fills up completely. Since the parallel walls are connected by the bottom of the wedge, no metastable states are expected[14].

- On approaching coexistence, the asymptotic behaviour described in (8) is preceded by pre-asymptotic regimes (apart from the above mentioned transitions for $\gamma \geq 2$). In this macroscopic limit, the asymptotic regime G_1 is preceded by a regime G_2 and the asymptotic regime G_2 is preceded by a regime G_1. These regimes are not only important in themselves but, as previous studies show [15], they can sometimes appear as the asymptotic ones for experimental or computational purposes.

All this features are shown in the phase diagram of Fig. 3. Along with a number of asymptotic and pre-asymptotic regimes (and the crossovers between them), geometry itself divides the phase diagram into three characteristic regions with one meniscus, two menisci or dry.

2.3 Geometrical Model

This rich scenario has to be modified by the inclusion of the fluid-substrate interaction. The macroscopic approach describes correctly the existence of capillary condensation and the presence of an asymptotic regime G_1 for $\gamma < 1$. However, it lacks information about microscopic effects and, therefore, wetting

is not recovered in the limit $\gamma \to 0$. Inclusion of these effects is a complex task, as shown in section 2.1. We opt here for including them in a simple geometrical manner. To do that, we proceed in two steps (See Fig. 4). First, we *coat* the solid substrate with a liquid layer of thickness ℓ_π by constructing a surface parallel to the substrate at every point. Then, we fit a cylinder of radius R_μ at the point of minimum curvature of *this* surface (instead of the original substrate). The resulting adsorbed layer is the continuous combination of the coating and the meniscus. Note that, with the inclusion of intermolecular forces (for this geometrical model, contained in the planar thickness ℓ_π), the phase diagram depends on the Hamaker constant and the range of the forces as parameters. In our calculations, we have considered the experimentally relevant case of dispersion forces $p = 2$. Besides, we have fixed the value of the dimensionless quantity $A/12\pi\sigma L^2 \sim 10^{-3}$. Considerably different values of this quantity modify the presence of pre-asymptotic regimes but do not introduce any new feature in the phase diagram. We stress here that this model, exact by construction in the macroscopic limit, does not intend to be a microscopic description of these systems but to capture the essential features of geometrically dominated adsorption, which, due to the lack of adequate models, remains largely unexplored.

The resulting phase diagram, shown in Fig. 5, is characterised by the following features:

- The asymptotic behaviour of the interface by approaching coexistence can be classified into *three* different regimes, determined by the shape of the substrate:

$$\ell_0 \sim \begin{cases} \Delta\mu^{-\beta_0} & 0 \le \gamma \le \gamma^* \\ \Delta\mu^{-\frac{\gamma}{2-\gamma}} & \gamma^* \le \gamma \le 1 \\ \Delta\mu^{-\gamma} & 1 \le \gamma, \end{cases} \tag{11}$$

  where $\gamma^* \equiv 2\beta_{co}/(1+\beta_{co})$. For $\gamma < 1$, this shows perfect agreement with

the results of the elaborate effective interfacial model (6) showing that geometry is largely responsible for the behaviour of the interface. For $\gamma > 1$, geometry dominates asymptotically and the inclusion of ℓ_π does not modify the macroscopic results. Notice that our particular case, $p = 2$, implies $\gamma^* = 1/2$.

- The phase diagram remains divided into three regions with zero, one or two menisci although the location of the transitions is shifted to higher values of $\Delta\mu$. The meniscus transition and the Moses transition are given implicitly by $R_\mu + \ell_\pi = \mathcal{R}(\hat{x})$ and $R_\mu + \ell_\pi = \psi(\bar{x}) + \bar{x}/\psi'(\bar{x})$ respectively, where ℓ_π represents a correction due to the thickness of the adsorbed layer ($\hat{x}$ and $\bar{x}$ remain the same). In the limit $\gamma \to \infty$, the correction given by ℓ_π happens to be the exact correction to the Kelvin equation for short-ranged forces. We mention here that both transitions turn into sharp crossovers when fluctuations effects, not discussed here, are taken into account [13].

- The pre-asymptotic regimes for $\gamma < 2$ differ from those obtained in the macroscopic approach and are strongly influenced by the presence of the microscopic layer. For $\gamma < 1$, we find a unique pre-asymtotic regime (GP) involving geometric and planar features for which the midpoint thickness grows like $\ell_0 \sim \Delta\mu^{-\gamma\beta_0}$. In contrast, for $1 < \gamma < 2$, the midpoint thickness grows in a planar manner. Note that these pre-asymptotic regimes have been determined by the sheer geometrical influence of the microscopic layer (comparable to the value of ℓ_0 in these regimes) and, therefore, a full inclusion of intermolecular forces could modify them significantly.

3 Conclusions

We show here that the adsorption properties of a substrate are strongly affected by the shape of its surface. To establish the connection between wetting and

capillary condensation, we have considered adsorption at substrates corresponding to generalised wedge geometries. By varying a parameter, this geometry smoothly changes from a planar substrate to a capillary slit. The influence of the substrate shape was found in a number of geometry-dominated asymptotic and pre-asymptotic regimes. Regarding the latter, it is important to mention that the appearance and merging of menisci plays an important role in the adsorption at *smooth* surfaces. These generalised wedges could be used as microfluidic devices to place mesoscopic amounts of liquid in preferential points of a solid surface in a controlled manner by simply varying the partial pressure. We anticipate that a similar phase diagram to the one presented here is expected for radially symmetric substrates ranging between a planar substrate and a capillary tube.

ACKNOWLEDGMENTS

CR acknowledges economical support from the European Commission under contract ERBFMBICT983229.

References

[1] S. Dietrich, in *Phase Transitions and Critical Phenomena*, (C. Domb and J.L. Lebowitz, eds.), Vol. **12**, p. 1 (Academic Press, London, 1988).

[2] J. Israelachvili, *Intermolecular & Surface Forces*, (Academic Press, London, 1991).

[3] Y. Xia and G.M. Whitesides, *Angew. Chem. Int. Ed.* **37** 550 (1998), M. Trau *et al.*, *Nature*, **390**, 674 (1997).

[4] R. Evans, U.M.B. Marconi and P. Tarazona, *J. Chem. Phys.* **84**, 2376 (1986).

[5] H.K. Christenson, *Phys. Rev. Lett.* **73**, 1821 (1994).

[6] E.H. Hauge, *Phys. Rev.* A **46**, 4994, (1992).

[7] K. Rejmer, S. Dietrich and M. Napiórkowski, *Phys. Rev.* E **60**, 4027 (1999).

[8] A.O. Parry, C. Rascón and A.J. Wood, *Phys. Rev. Lett.* **83**, 5535 (1999).

[9] A.O. Parry, C. Rascón and A.J. Wood, *Phys. Rev. Lett.* (to be published), `cond-mat/9911431`.

[10] C. Rascón and A.O. Parry, *J. Chem. Phys.* **112**, 5175 (2000).

[11] C. Rascón and A.O. Parry, (to be published).

[12] See, for instance, M.O. Robbins, D. Andelman and J.-F. Joanny, *Phys. Rev.* A **43** 4344 (1991).

[13] C. Rascón and A.O. Parry (in preparation).

[14] U.M.B. Marconi and F. Van Swol, *Phys. Rev.* A **39**, 4109 (1989).

[15] E. Carlon, A. Drzewiński and J. Rogiers, *Phys. Rev.* B **58**, 5070 (1998).

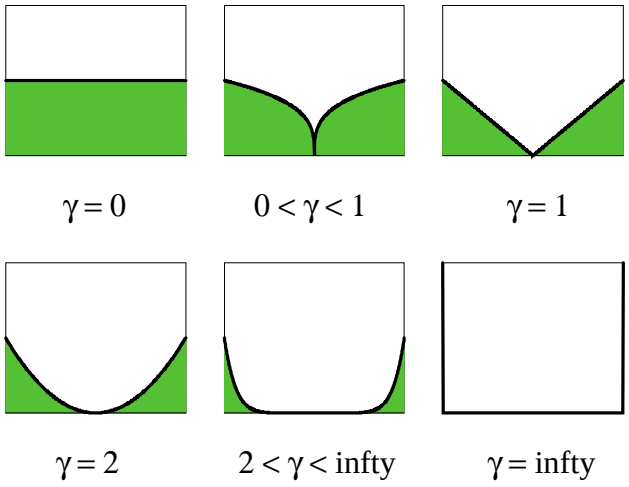

Figure 1: Cross section of the generalised wedge geometry for different values of the parameter γ. By varying this parameter, it is possible to change smoothly the shape of a planar substrate ($\gamma = 0$) to that of a capillary slit ($\gamma = \infty$).

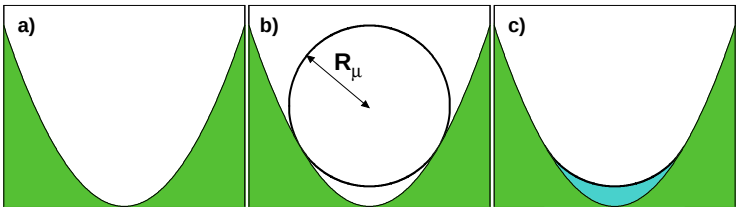

Figure 2: Geometrical construction to determine the macroscopic meniscus. This particular case is a parabolic wedge (a). A cylinder of radius R_μ is fitted in the wedge (b). The tangency points constitute the edges of the meniscus (c).

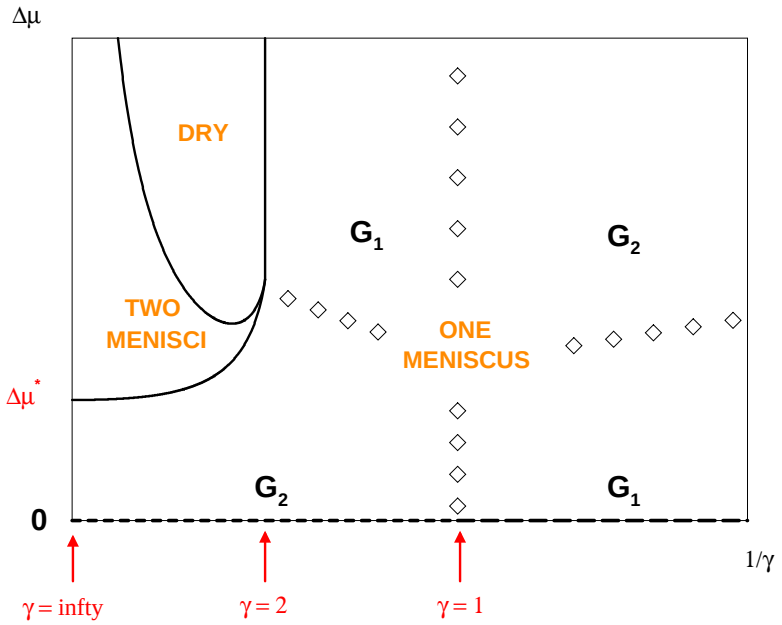

Figure 3: Schematic phase diagram showing *macroscopic* adsorption in different types of generalised wedges ignoring the influence of microscopic fluid-substrate interaction. Aproaching bulk liquid-gas coexistence ($\Delta\mu \to 0$), two asympotic regimes take place: G_1 for $\gamma < 1$ and G_2 for $\gamma > 1$. Preceding these regimes, three pre-asymptotic regimes are obtained: G_2 for $\gamma < 1$, G_1 for $1 < \gamma < 2$ and a sequence of two phase transitions for $\gamma > 2$ (solid lines) related to the formation of two menisci and their merging (see text). Note that capillary condensation is recovered for $\gamma \to \infty$. The diamonds represent crossovers between regimes.

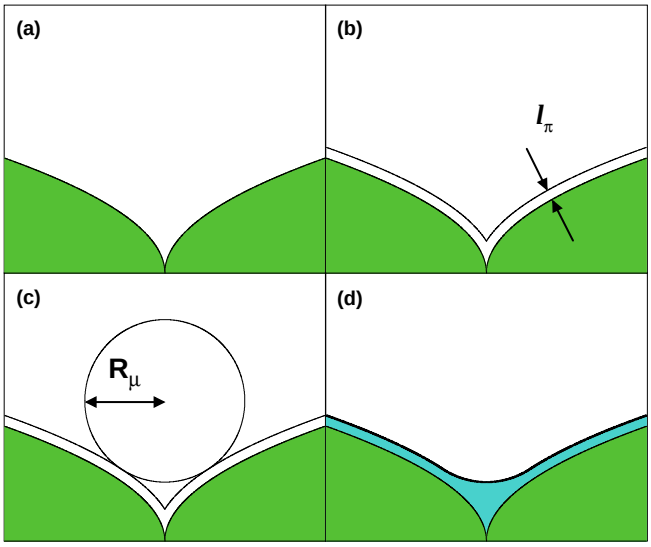

Figure 4: Geometrical construction to determine the shape of the microscopic interface. In this particular case, $\gamma < 1$ (a). First, the substrate is *coated* with a layer of thickness ℓ_π (b). Then, a cylinder of radius R_μ is fitted in the wedge (c). The final shape is given by the continous combination of both shapes (d)

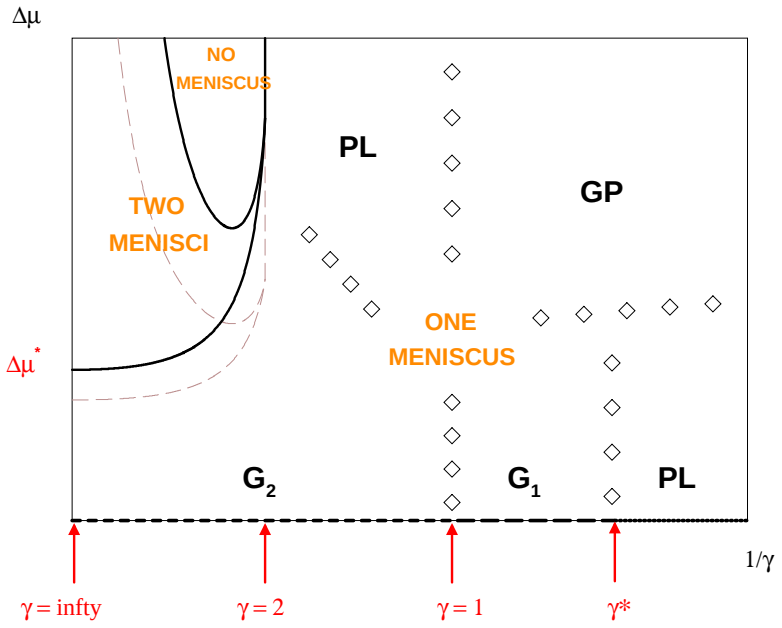

Figure 5: Schematic phase diagram of adsorption at generalised wedges calculated with a geometrical model for $p=2$ and $A/12\pi\sigma\, L^2 \sim 10^{-3}$ (analogous to Fig. 3). We find *three* asympotic regimes: planar (PL) for $0<\gamma<\gamma^*$, G_1 for $\gamma^*<\gamma<1$ and G_2 for $\gamma>1$. Preceding these, three pre-asymptotic regimes are observed: GP for $\gamma<1$, PL for $1<\gamma<2$ and a sequence of two transitions for $\gamma>2$ (see text). These have been shifted with respect to those obtained by a purely macroscopic approach (thin dashed lines). The diamonds represent crossovers between regimes.